

Agrin Inhibition in Enteric Neural Stem Cells Enhances Their Migration Following Colonic Transplantation

Jessica L. Mueller¹, Rhian Stavelly¹, Richard A. Guyer¹, ^{ORCID}Ádám Soos,² Sukhada Bhave¹, Chris Han¹, Ryo Hotta¹, ^{ORCID}Nandor Nagy^{*2}, Allan M. Goldstein^{*1}

¹Department of Pediatric Surgery, Massachusetts General Hospital, Boston, MA, USA

²Department of Human Morphology and Developmental Biology, Faculty of Medicine, Semmelweis University, Budapest, Hungary

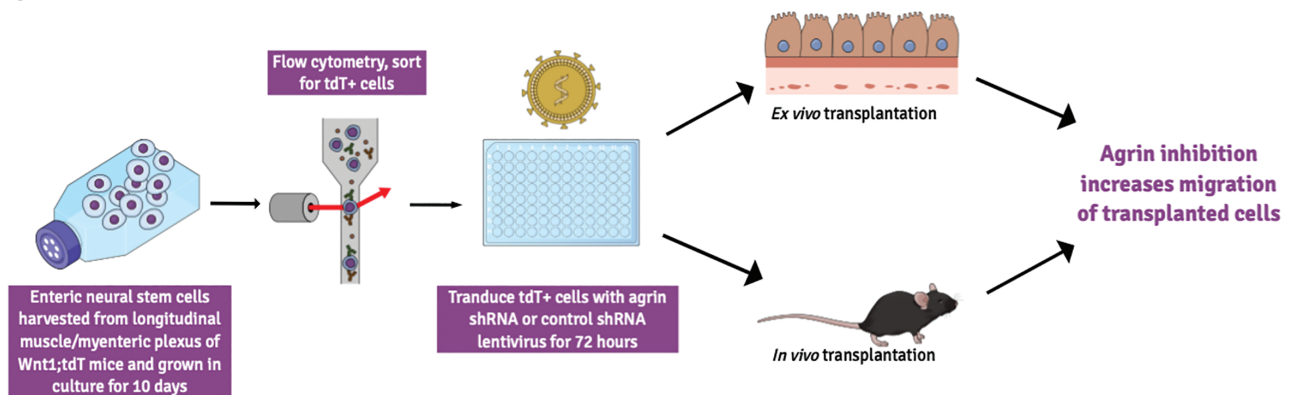
*Corresponding author: Allan M. Goldstein, MD, Department of Pediatric Surgery, Warren 1151, Massachusetts General Hospital, 55 Fruit Street, Boston, MA 02114, USA. Email: amgoldstein@mgh.harvard.edu; or, Nandor Nagy, PhD, Semmelweis University, Tuzolto St. 58, Budapest 1094, Hungary. Fax: 36 1 2153064; Email: nagy.nandor@semmelweis.hu

Abstract

Regenerative cell therapy to replenish the missing neurons and glia in the aganglionic segment of Hirschsprung disease represents a promising treatment option. However, the success of cell therapies for this condition are hindered by poor migration of the transplanted cells. This limitation is in part due to a markedly less permissive extracellular environment in the postnatal gut than that of the embryo. Coordinated interactions between enteric neural crest-derived cells (ENCDCs) and their local environment drive migration along the embryonic gut during development of the enteric nervous system. Modifying transplanted cells, or the postnatal extracellular environment, to better recapitulate embryonic ENCDC migration could be leveraged to improve the engraftment and coverage of stem cell transplants. We compared the transcriptomes of ENCDCs from the embryonic intestine to that of postnatal-derived neurospheres and identified 89 extracellular matrix (ECM)-associated genes that are differentially expressed. Agrin, a heparin sulfate proteoglycan with a known inhibitory effect on ENCDC migration, was highly over-expressed by postnatal-derived neurospheres. Using a function-blocking antibody and a shRNA-expressing lentivirus, we show that inhibiting agrin promotes ENCDC migration in vitro and following cell transplantation ex vivo and in vivo. This enhanced migration is associated with an increased proportion of GFAP + cells, whose migration is especially enhanced.

Key words: stem cell therapy; enteric neuronal stem cells; enteric nervous system; extracellular matrix; Hirschsprung disease.

Graphical Abstract



Significance Statement

The success of stem cell therapy as a treatment for Hirschsprung disease requires a permissive extracellular environment, which can be achieved by modifying stem cells to make them more migratory and resemble embryonic enteric neural crest-derived cells. We compared the transcriptome of enteric neural crest-derived cells from the embryonic intestine and postnatal neurospheres and identified elevated expression of agrin as a potential hindrance to stem cell migration. By silencing agrin in enteric neuronal stem cells, their migration was significantly enhanced in culture and following transplantation. This is the first study to directly modify stem cells for the treatment of ENS disease.

Received: 21 July 2023; Accepted: 5 January 2024.

© The Author(s) 2024. Published by Oxford University Press.

This is an Open Access article distributed under the terms of the Creative Commons Attribution-NonCommercial License (<https://creativecommons.org/licenses/by-nc/4.0/>), which permits non-commercial re-use, distribution, and reproduction in any medium, provided the original work is properly cited.

For commercial re-use, please contact reprints@oup.com for reprints and translation rights for reprints. All other permissions can be obtained through our RightsLink service via the Permissions link on the article page on our site—for further information please contact journals.permissions@oup.com.

Introduction

Congenital or acquired disruption of the enteric nervous system (ENS) leads to various neurointestinal diseases, including Hirschsprung disease, esophageal achalasia, gastroparesis, and others. These diseases have significant morbidity and limited treatment options. Stem cell therapy represents a potential therapeutic strategy to replace the missing ENS,¹⁻³ but its success to date has been limited, largely due to inadequate migration of transplanted cells in the recipient gut.⁴⁻⁶ Embryonic development of a functional ENS relies on interactions between enteric neural crest-derived cells (ENCDCs) and the extracellular matrix (ECM) through which they migrate within the gut mesenchyme.⁶ These interactions ensure appropriate and well-timed cell migration, proliferation, and differentiation into the enteric neurons and glia that regulate numerous gastrointestinal processes, including both motor and sensory functions. Many studies have demonstrated the important influence of ECM proteins on ENCDC migration. Laminin,⁷ fibronectin,⁸⁻¹⁰ vitronectin,¹⁰ collagen 18,¹¹ tenascin-C,⁹ and ECM binding proteins, including N-cadherin and β 1-integrins,¹² have all been shown to promote ENCDC migration. Conversely, agrin,¹¹ collagen VI,¹³ and chondroitin sulfate proteoglycans, including versican and collagen IX,¹⁴⁻¹⁷ prevent migration, highlighting the critical role of the ECM in ENS formation.

Hirschsprung disease, one of the best understood neurointestinal diseases, is caused by the failure of ENCDCs to complete their rostrocaudal migration during embryonic development.⁶ This migratory failure can be due to intrinsic defects in ENCDCs and/or insufficient signals from the surrounding environment.¹⁸ In Hirschsprung disease, incomplete colonization of the intestine by ENCDCs results in a variable length of distal intestinal aganglionosis, always involving the rectosigmoid colon, and affecting 1/5000 live births.¹⁹ While surgical removal of the aganglionic segment remains the primary treatment for Hirschsprung disease, it is associated with short- and long-term risks.^{20,21} Many patients experience persistent bowel dysfunction after surgery, including incontinence, constipation, and enterocolitis.²²⁻²⁷ Transplanting ENS cells to replace the missing neurons and glia in the aganglionic segment would address the underlying aganglionic pathology of Hirschsprung disease and preclude the need for surgery, making this a prime focus of current Hirschsprung disease research.¹⁸

ENCDCs have been isolated from the small and large intestines,²⁸ from full thickness tissue and mucosa alone,²⁹ from neonates,^{3,30} children,³¹ and adults,³² and even from the aganglionic segment of patients with Hirschsprung disease.³³ These cells proliferate in culture and expand exponentially to form free-floating neurospheres,^{1,31,32,34} which are capable of differentiating into neurons and glial cells when transplanted into the embryonic gut.³⁴ However, poor engraftment, migration, and proliferation of transplanted cells have limited their success.^{5,6,35} A major obstacle has been the postnatal gut environment, which is markedly less permissive to ENCDCs than the embryonic gut.^{36,37} To optimize stem cell delivery and efficacy, ENCDCs can be directly modified using viral vectors^{38,39} or can be co-administered with growth-promoting molecules delivered by co-injection⁴⁰ or packaged in nanoparticles.^{41,42}

Given the important role of coordinated interactions between ENCDCs and their local environment, the success of stem cell transplantation as a regenerative therapy requires a

permissive postnatal gut environment. Notably, the extracellular matrix in Hirschsprung disease is different from that of a normal healthy colon.^{11,43-45} It would be extraordinarily challenging to develop therapies that modify the vast changes of that extracellular milieu. We therefore chose to directly modify the stem cells prior to transplantation with the goal of optimizing their migration within the extracellular gut environment. This approach represents a clinically feasible and relevant therapeutic cell-based strategy for the treatment of Hirschsprung disease and potentially other neurointestinal diseases.

Materials and Methods

Single-Cell Analysis

Published datasets by Morarach et al⁴⁶ and Guyer et al⁴⁷ were utilized for analysis. Mouse embryonic datasets at E15.5 and E18.5⁴⁶ were downloaded from the NCBI Sequence Read Archive. Runs SRR11635571, SRR11635572, and SRR11635573 were obtained using the SRA Toolkit “fastq-dump” command. Genome alignment and feature-barcode matrix generation were executed with the Cell Ranger “cellranger count” command on the Mass General Brigham ERISOne Research Computing Cluster. Subsequent analysis was performed in the R environment (RStudio Version 2023.03.0 + 386) with Seurat. The datasets were filtered with the removal of cells expressing a number of genes more than one standard deviation away from the mean and the removal of cells with greater than 10% mitochondrial genes. This filtration removes low-quality or dying cells, empty droplets, and doublets or multiplets from the dataset. Embryonic progenitors were selected based on high *Sox10* expression (clusters 0, 2, 5, 9), labeled “embryonic progenitors,” and included in further analyses.

Dataset on postnatal-derived neurospheres was provided by Guyer et al⁴⁷. The dataset was filtered as the authors describe, with the removal of cells expressing a number of genes more than one standard deviation away from the mean and removal of cells with greater than 10% mitochondrial genes. Progenitor cells were selected based on high *Sox10* and *Gfap* expression as was done in the original paper, with clusters 0, 1, 2, 3, 4, 6, 8, and 14 labeled “neurosphere progenitors” and included in subsequent analyses.

The embryonic progenitor and neurosphere progenitor datasets were integrated using the “FindIntegrationAnchors” command in Seurat.⁴⁸ After integration, principle component analysis (PCA) was performed. Neighbors were identified and uniform manifold approximation and projection (UMAP) dimensional reduction was performed using the first 30 principal components. Clusters were identified using the “FindClusters” command with resolution = 0.5 using the Louvain algorithm.⁴⁹ Differential gene expression analysis was performed using the R package DESeq2.⁵⁰ Genes with log₂ fold changes > 0.5, percent expression > 25%, and adjusted *P*-value < .001 were considered significant. Statistically significant genes were then compared to a Gene Ontology Extracellular Matrix dataset (GO: 0031012; 530 genes) to identify significant ECM genes.

Animals

This study was performed according to experimental protocols approved by the Institutional Animal Care and Use Committees of Massachusetts General Hospital.

Wnt1^{Cre/+} mice (B6.Cg-*H2az*2^{Tg(Wnt1-cre)11Rth} Tg(Wnt1-GAL4)11Rth/JStock # 009107), *R26R-tdT* reporter mice (B6.Cg-*Gt(ROSA)26Sor*^{tm14(CAG-tdTomato)Hze}J; Stock #007914), C57BL/6J (Stock #000664), and B6;129-*Ednrb*^{tm1Yua}/J (Stock#003295) were obtained from Jackson Laboratory (Bar Harbor, ME, USA). *Wnt1*^{Cre/+} mice were crossed with *R26R-tdT* reporter mice to generate *Wnt1-Cre*⁺;*R26-tdT* mice (annotated as *Wnt1;tdT*). *Ednrb* heterozygotes were bred to generate *Ednrb* knockout mice (*Ednrb*^{-/-}) which demonstrate distal colonic aganglionosis akin to human Hirschsprung disease. All mice were housed and bred at the Center for Comparative Medicine animal facility at Massachusetts General Hospital under specific pathogen-free conditions.

Embryos

Fertilized White Leghorn chicken (*Gallus gallus domesticus*) eggs were obtained from commercial breeders (Prophyl-BIOVO Ltd., Hungary) and maintained at 37.5 °C in a humidified incubator (HEKA 1 + egg incubator, Rietberg, Germany). Avian embryos were staged according to the number of embryonic days (E) and the gut development stages were referenced to the chick embryo gut staging table⁵¹ and the ENS formation timetable.⁵² All animal experiments were approved by the Animal Experimentation Review Board of Semmelweis University.

In Vitro Tissue Recombination and Chorioallantoic Membrane (CAM) Transplants

To study the contribution of the mouse neurospheres to the avian hindgut ENS chorioallantoic membrane (CAM) transplantation was performed. Using tungsten needles, preganglionic hindgut grafts were prepared by removing the cloacal region and the nerve of Remak from the hindgut of E5 (Hamburger-Hamilton (HH) stage 26) chick embryos. Under stereomicroscope visualization, two *Wnt1;tdT* mouse-derived neurospheres of embryonic or adult origin were implanted into each of the ceca of the E5 chick embryo. These chick-mouse chimeric recombinants were then transplanted onto the CAM of E9 (HH 35) chick embryos and cultured for 8 days as described.¹¹ At the conclusion of this culture period, the explants were excised, fixed overnight in 4% paraformaldehyde (PFA) at 4 °C, and embedded for cryosectioning. Migration distance was assessed by counting the farthest cell away from the transplanted region in multiple sections.

Generation of Neurospheres

Mice were euthanized and their small intestine was removed from duodenum to terminal ileum. The longitudinal muscle-myenteric plexus (LMMP) layer was dissected from underlying tissue in PBS and digested for 60 minutes at 37 °C in dispase (250 µg/mL; STEMCELL Technologies) and collagenase XI (1 mg/mL; Sigma-Aldrich). Following digestion, the cells were filtered through a 70-µm filter and resuspended at a density of 50 000 cells/mL with a total volume of 10 mL placed in 25 cm flasks (Corning Inc.). Neuroproliferation media contained penicillin and streptomycin (1%; Life Technologies, Thermo Fisher Scientific), B27 Supplement (1x; Gibco, Thermo Fisher Scientific), N-2 Supplement (1x; Gibco, Thermo Fisher Scientific), basic fibroblast growth factor (20 ng/mL; Stemcell Technologies), insulin-like growth factor 1 (20 ng/mL; Thermo Fisher Scientific), retinoic acid (75 ng/mL; Sigma-Aldrich), and 2-mercaptoethanol (50 µmol/L;

Gibco, Thermo Fisher Scientific) in equal parts Neurocult Mouse Basal Medium (STEMCELL Technologies) and Dulbecco's Modified Eagle Medium (DMEM; Gibco, Thermo Fisher Scientific). These primary neurospheres were cultured at 37 °C and 5% CO₂ for 10 days.

Primary neurospheres were then prepared for cell sorting. They were dissolved for 45 minutes into a single-cell suspension using accutase (STEMCELL Technologies), filtered through a 40-µm filter, and stained with DAPI. Cells were then sorted as described below and tdT + cells were kept and manually counted with Trypan blue to assess number and viability. tdT + cells were then plated in a 96-well round bottom ultra-low attachment dish (Corning Incorporated) at a density of 25 000 cells/mL for ex vivo and in vivo experiments and 50 000 cells/mL for in vitro experiments.

Cell Sorting

Cell sorting was performed on the Massachusetts General Hospital campus by the Harvard Stem Cell Institute's Center for Regenerative Medicine Flow Cytometry Core, utilizing BD Biosciences (Franklin Lakes) FACS Aria sorting instruments. Cells were sorted for tdT positivity (indicating *Wnt1* expression) and DAPI negativity (indicating live cells). Approximately 30% of cells were live and expressed tdT.

Transduction With Lentivirus

Immediately after cell sorting, tdT + cells were transduced with an agrin shRNA lentivirus containing 4 unique 29mer agrin targeting shRNA and a GFP reporter (purchased from Origene; CAT#: TL512313V, and expanded and packaged at the MGH Vector Core Facility, Massachusetts General Hospital Neuroscience Center, Charlestown, MA to have a final concentration of 10¹² TU/ml) or a control scramble shRNA with a GFP reporter (purchased from Origene; CAT# TR30021V, and expanded and packaged at the MGH Vector Core Facility to have a final concentration of 10¹² TU/mL). After testing various multiplicities of infection (MOI), an MOI of 90 was utilized for both viruses, and we observed a transduction efficiency of 50%-60% for the agrin shRNA lentivirus and 25%-30% for the control shRNA lentivirus. At this concentration, we observed no toxicity. Cells were transduced for 72 hours.

Cell Migration, Proliferation, and Differentiation Assays

As described above, sorted tdT + cells were plated in a 96-well dish at a concentration of 50 000 cells/mL (migration assay) or 12 500 cells/mL (proliferation/differentiation assay) and cultured for 72 hours. Neurospheres utilized in the migration assay were therefore uniform in size and contained 10 000 cells. Similarly, neurospheres utilized in the proliferation and differentiation assays were uniform in size and contained 2500 cells. A smaller number of cells were utilized to be able to differentiate individual cells via immunohistochemistry. After 72 hours, single neurospheres were transferred onto fibronectin-coated dishes (1:200 in PBS, Sigma-Aldrich).

In the migration assay, neurospheres were cultured in either DMEM-only or DMEM with agrin function-blocking antibody (20 µg/mL, MAB5204, Millipore) for 72 hours and then imaged as described above. This concentration was chosen based on prior published work from our lab.¹¹ Cell migration was assessed utilizing ImageJ software v1.53t using binary thresholding to determine the total area covered by tdT + cells.

Given that all neurospheres started with the same number of tdT + cells, this migration method considers both the distance and density of cell migration. To explain further, when cells do not migrate away from the neurosphere, the area covered by tdT + cells is small, and as cells start to migrate away the area of cell spread increases. However, if only the distance of cell migration is considered, a neurosphere that had one individual cell migrate a certain distance away from the center of the neurosphere would get the same value as a neurosphere that had many cells migrate that same distance. We therefore felt that the total area covered was a better metric for migration than just looking at distance alone.

In the proliferation and differentiation assays, neurospheres were cultured under control conditions (DMEM only) or experimental conditions (DMEM with 20 µg/mL of agrin function-blocking antibody) for 96 hours on fibronectin and then tissue was fixed for 30 minutes using 4% PFA. For the proliferation assay, neurospheres were treated with 10 µM EdU (Invitrogen, A10044) after 72 hours and imaged 24 hours later.

After fixation, the Click-iT EdU Cell Proliferation Kit for Imaging (Fisher Scientific, C10340) was used per the manufacturer's protocol. Cell nuclei were stained with DAPI (Invitrogen D1306). Immunostaining was also performed using GFAP, Calretinin, and nNOS as described below. Images were obtained using a Keyence BZX-700 All-In-One microscope. Proliferation and differentiation were determined by counting the number of tdT + cells that costained for EdU or GFAP, Calretinin, and nNOS, respectively. Given that there were varying numbers of each type of differentiated cell per preparation, assessment of migration using the total area of cell spread would not be an accurate measurement of migration. Therefore, the migration of different types of cells was assessed using the octant method.² Briefly the image was divided into octants and the distance was measured between the center of the neurosphere and to the farthest fluorescently labeled cell in each octant. The average distance was calculated to represent the migration distance in each preparation.

Ex Vivo and In Vivo Transplantation

Ex vivo transplants were performed onto colonic LMMP peeled and isolated from either C57BL/6J or Ednrb^{-/-} mice. Adult (4- to 12-week old) C57BL/6J mice or 2-week old Ednrb^{-/-} mice were sacrificed using CO₂ asphyxiation. The colon was removed, opened longitudinally, and washed with PBS. The LMMP was peeled away from the lamina propria under a dissecting microscope and pinned into a Sylgard coated dish. For the Ednrb^{-/-} mice, only the distal 2 centimeters were utilized to ensure colonic aganglionosis. Using fine forceps, a small pocket was created in the muscularis propria and a single previously sorted and transduced neurosphere was transplanted into the pocket. This tissue was then cultured for 7 days in media consisting of 5% fetal bovine serum (FBS, Sigma-Aldrich) and 1% anti-anti (antibiotic-antimycotic, containing penicillin, streptomycin, and amphotericin B, Gibco) in DMEM. After 7 days tissue was fixed for 4-6 hours in 4% PFA and images were obtained.

Only C57BL/6J mice were utilized for *in vivo* transplants. Adult (4- to 12-week-old) C57BL/6J mice were anesthetized utilizing inhaled isoflurane (1%-4%). A mini laparotomy incision was made and the distal colon was exposed. Two small subserosal pockets were created using fine forceps

approximately 0.5 cm apart, and in each pocket a single previously sorted and transduced neurosphere was placed. Mice were then returned to the animal facility according to protocol and sacrificed using CO₂ asphyxiation seven days after transplantation.

Immunohistochemistry and Image Processing

Immunohistochemistry was performed as previously described.⁵² For cryosections, tissue was fixed in 4% PFA for 1 hour, then incubated with 15% sucrose overnight at 4 °C, infiltrated with 7.5% gelatin/15% sucrose in PBS for 1 h at 37 °C, then rapidly frozen at -50 °C in methylbutane. Twelve micrometer-thick cryosections were stained using the following primary antibodies: anti-HuC/D (clone: 16A11, 1:50, Thermo Fisher Scientific, A-21271), which recognizes a neuron-specific RNA-binding protein; rabbit anti-S100B calcium-binding protein B specific for mouse enteric glia (RB087A1, S100; 1:50; NeoMarkers), and anti-mouse Agrin (1:50; R&D Systems, AF550). Primary antibodies were applied for 45-90 min, followed by Alexa-conjugated fluorescent secondary antibodies: Alexa Fluor 488 goat anti-mouse IgG (1:200, A32723), Alexa Fluor 488 goat anti-rabbit IgG (1:200, A32731) and Alexa Fluor 488 donkey anti-goat (1:100, A11055), all from Thermo Fisher Scientific. Cell nuclei were stained with DAPI. The sections were covered by aqueous Poly/Mount. Section images were recorded using a Nikon Eclipse E800 fluorescence microscope and a Zeiss LSM 710 confocal microscope.

For whole-mount immunofluorescent staining, colons were fixed overnight in 4% PFA at 4 °C, permeabilized with 1% normal goat serum and 0.1% Triton X-100 (Sigma-Aldrich, 9036-19-5) in PBS overnight at 4 °C. Specimens were labeled overnight with anti-Agrin (1:50; R&D Systems, AF550) or mouse anti-tubulin β3 (Tuj1, 1:400, conjugated to Alexa Fluor 647, BioLegend) at 4 °C. After washing in PBS, fluorescent secondary antibody (Alexa Fluor 488 donkey anti-goat, 1:100, A11055) was applied for 1 hour. Whole-mount images were recorded using a Nikon SMZ25 (with Prior L200/E unit) fluorescence stereomicroscope.

For staining of cells, cells were fixed for 30 minutes in 4% PFA at 4 °C, permeabilized in 0.1% Triton X-100 for 20 minutes, washed with PBS, and blocked with 10% donkey serum for 1 hour at room temperature. Primary antibodies were diluted in 10% donkey serum, which included GFAP (1:500, Abcam ab53544), Calretinin (1:200, Invitrogen 18-0211), nNOS (1:400, Invitrogen 61-7000), and incubated overnight at 4 °C. Secondary antibodies were diluted in 10% donkey serum, which included donkey anti-goat IgG (1:200, conjugated to Alexa Fluor 555, Invitrogen) and donkey anti-rabbit IgG (1:200, conjugated to Alexa Fluor 488, Invitrogen) and incubated at room temperature for 2 hours. Cell nuclei were counterstained with DAPI solution (Invitrogen). Images were obtained with a Keyence BZX-700 all-in-one microscope and analyzed using ImageJ software v1.53t.

Image processing, including tiling and merging of pseudocolored immunofluorescent images, used CellSens, ZEISS ZEN Imaging, Nis-Elements (v 5.02) Imaging proprietary software, and ImageJ software v1.53t (National Institutes of Health, Bethesda, MD, USA, <http://rsb.info.nih.gov/ij/>). The area of cell spread was quantified through binary thresholding of fluorescent cells to designate an area of interest.

Statistical Analysis

Analyses were performed using R Studio and GraphPad Prism software (Graph-Pad, CA, USA). For pairwise comparisons, a Mann-Whitney test was performed. Comparisons of migration were performed using unpaired 2 sample *t*-tests when only one batch was utilized, or 2-way ANOVA accounting for batch effect when multiple experiments were included in the analysis. *P*-values < .05 were considered statistically significant. Bar graphs are presented with the mean and standard error of the mean (SEM) bars.

Results

Comparative Single Cell Analysis Reveals a Non-Permissive ECM Transcriptome in Postnatal Enteric Neurospheres

The previously published E15.5 and E18.5 murine ENS scRNA-seq dataset⁴⁶ (Fig. 1A) was restricted to clusters of progenitor cells based on their *Sox10* expression, indicative of ENS progenitors. This includes clusters 0, 2, 3, and 9, which we label “embryonic progenitors” (Fig. 1B, 1C). The dimensional reduction was also performed on postnatal-derived neurospheres from a dataset published by Guyer et al⁴⁷ (Fig. 1D) and restricted to progenitor cells based on their expression of *Sox10* (Fig. 1E) and Glial fibrillary acidic protein (*Gfap*) (Fig. 1F). Clusters 0, 1, 2, 3, 4, 6, 8, and 14 were included in the analysis and labeled “neurosphere progenitors” (Fig. 1D, box). Differential gene expression analysis between the embryonic progenitors (Fig. 1B) and postnatal neurosphere progenitors (Fig. 1D) was performed and compared to a curated Gene Ontology ECM database. This analysis identified 89 differentially expressed ECM genes across the 2 groups (Supplementary Table S1).

We next compared the expression of genes encoding proteins that have been studied in the neural crest, including various pro-migratory, inhibitory, and epithelial-to-mesenchymal transition (EMT) genes to identify specific targets for further research. The ECM transcriptome of postnatal neurospheres revealed low expression of selected pro-migratory genes, including laminin beta 1 (*Lamb1*) and its receptor (laminin receptor; *Lamr*),⁵³ which could contribute to their limited migration. Other promigratory genes, including laminin beta 2 (*Lamb2*), laminin subunit alpha 5 (*Lama5*), tenascin C (*Tnc*), integrin subunit beta 1 (*Itgb1*), and collagen 18 alpha 1 subunit (*Col18a1*), are strongly expressed by postnatal derived neurospheres (Supplementary Fig. S1A). Importantly, we noted over-expression of multiple genes known to inhibit neural crest cell migration, including collagen VI (*Col6a1*) and agrin (*Agrn*), by postnatal neurospheres. Other inhibitory molecules, including the alpha 2 and alpha 3 subunits of collagen 9, have low levels of expression in postnatal neurospheres (Supplementary Fig. S1B). Selected EMT genes with known promigratory roles, including members of the “a disintegrin and metalloproteinase” (ADAM) family (*Adamts5*, *Adamts1*, *Adam10*) and the metalloproteinase (MMP) family (*Mmp2* and *Mmp17*), are expressed by both embryonic progenitors and postnatal neurospheres (Supplementary Fig. 1C). A dot plot shows the relative differential expression of these genes between embryonic and postnatal progenitors (Fig. 1G). Either the pro-migratory genes that are under-expressed, such as laminin beta 1 and its receptor, or the inhibitory

molecules that are over-expressed, including collagen VI and agrin, represent potential targets for optimizing cell migration following transplantation. Since agrin has previously been shown to inhibit the migration of neural crest cells in multiple contexts,⁵⁴ including during ENS development,¹¹ we chose agrin for further study.

Agrin, a secreted heparin sulfate proteoglycan (HSPG) that is inhibitory to neural crest cell migration, has significantly higher levels of normalized, log-transformed expression in postnatal derived neurospheres than in embryonic progenitors (Fig. 1H, 2.12 vs 0.79 respectively, *P* < .0001). Furthermore, agrin is expressed by 86% of neurosphere progenitor cells versus 40% of embryonic progenitor cells. Given its known role in ENCC migration during ENS development, agrin over-expression could be inhibitory to the migration of transplanted ENCCs. We therefore hypothesized that inhibition of agrin in ENCCs will enhance cell migration following transplantation of enteric neurospheres into the postnatal gut environment.

Postnatal, But Not Embryonic, Neurospheres Express Agrin, Which Inhibits ENCC Migration Following Implantation Into Embryonic Chick Intestine

Wholemounts of the longitudinal muscle/myenteric plexus (LMMP) of 3-week-old Wnt1;tdT mouse intestine strongly express agrin in the myenteric plexus (Fig. 2A). Agrin expression is specific to the cells of the myenteric plexus (Fig. 2B), forming part of an ECM capsule surrounding the ganglia. Neurospheres generated from this postnatal tissue highly express agrin (Fig. 2C'). Figure 2D shows a magnified section of the postnatal neurosphere. In contrast, embryonic midgut from E11.5 Wnt1;tdT mice reveals markedly decreased agrin expression (Fig. 2E). Magnified image (Fig. 2F) shows that Wnt1;tdT cells in the embryo do not produce agrin. Similarly, neurospheres generated from embryonic intestine have diminished agrin expression (Fig. 2G). Mean pixel intensity analysis of immunohistochemistry images demonstrates a significantly increased fluorescence corresponding to agrin production in neurospheres derived from postnatal versus embryonic tissue (190.5 vs 78.9, *P* < .001).

Postnatal neurospheres were generated from 3-week-old Wnt1;tdT mice and implanted into E5 chick ceca (Fig. 3A), which are aneural at this stage. The chick gut was then grafted onto the chorioallantoic membrane (CAM) for 8 days to allow time for the cells to migrate. At the end of the culture period, Wnt1 + ENCCs (Fig. 3B) can be seen expressing agrin (Fig. 3C) and exhibiting very limited cell migration (Fig. 3B). Figure 3D shows a magnified image of the implanted region. In contrast, similar implantation of Wnt1;tdT neurospheres prepared from embryonic mouse intestine into the chick ceca results in robust ENCC migration (Fig. 3E), with minimal agrin expression observed (Fig. 3F), and colonization of the entire host ENS with enteric glia (S100; Fig. 3G) and neurons (HU; Fig. 3H). Wnt1;tdT + fibers were seen to project significantly farther after implantation of embryonic versus adult neurospheres (Fig. 3I, 1184 mm vs 228.1 mm, *P* < 0.0001).

Agrin Blockade Increases Cell Migration In Vitro

Sorted tdT + neurospheres derived from 4-12 week-old Wnt1;tdT mice were cultured on fibronectin in DMEM only (Fig. 4A) or DMEM supplemented with an agrin

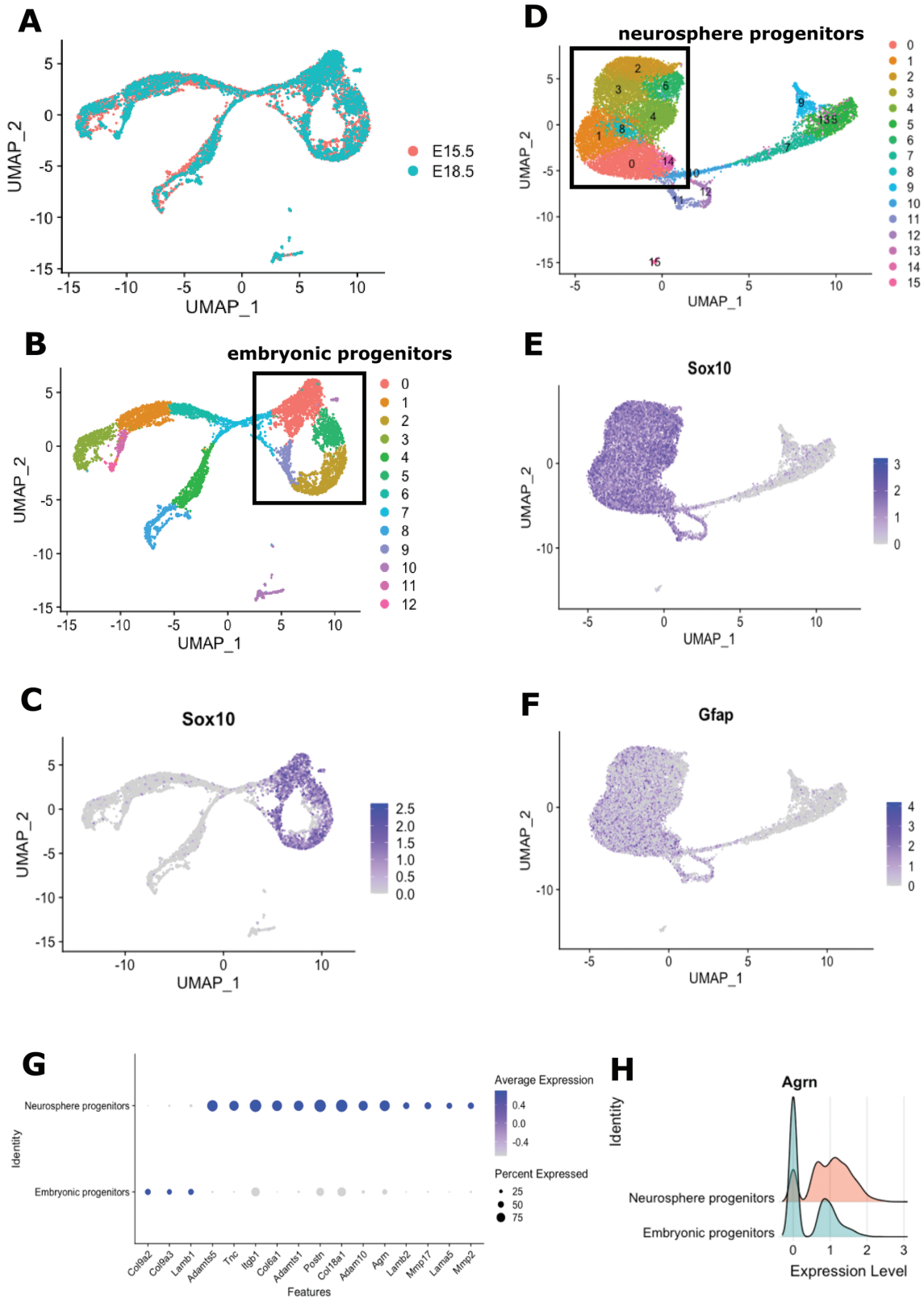


Figure 1. The ECM transcriptome is more permissive to cell migration in embryonic progenitors compared to postnatal-derived neurospheres. Uniform Manifold Approximation and Projection (UMAP) shows combined E15.5 and E18.5 murine embryonic ENS datasets (A), using data published by Morarach et al (2021), with dimensional reduction performed (B). Feature plot of *Sox10* expression (C) used to select cells consistent with “embryonic progenitors” (clusters 0, 2, 5, 9 with high *Sox10* expression) which are included in subsequent analysis. UMAP of 15,426 GFP + cells isolated from neurospheres generated from small intestine of 12-16 week-old Plp1^{GFP} mice (D), using data published by Guyer et al. (2023). Feature plots of *Sox10* (E) and *Gfap* (F) expression are shown to highlight progenitors. Clusters with high *Sox10* and *Gfap* are labeled “neurosphere progenitors” and selected for subsequent analysis. Expression of differentially expressed ECM genes between groups is shown on a dot plot (G), with dot size indicating the percentage of cells in each cluster with >0 transcripts detected, and color indicating relative level of gene expression. A ridge plot of *agrin* expression in neurosphere progenitors and embryonic progenitors shows higher levels of *agrin* in the former (H).

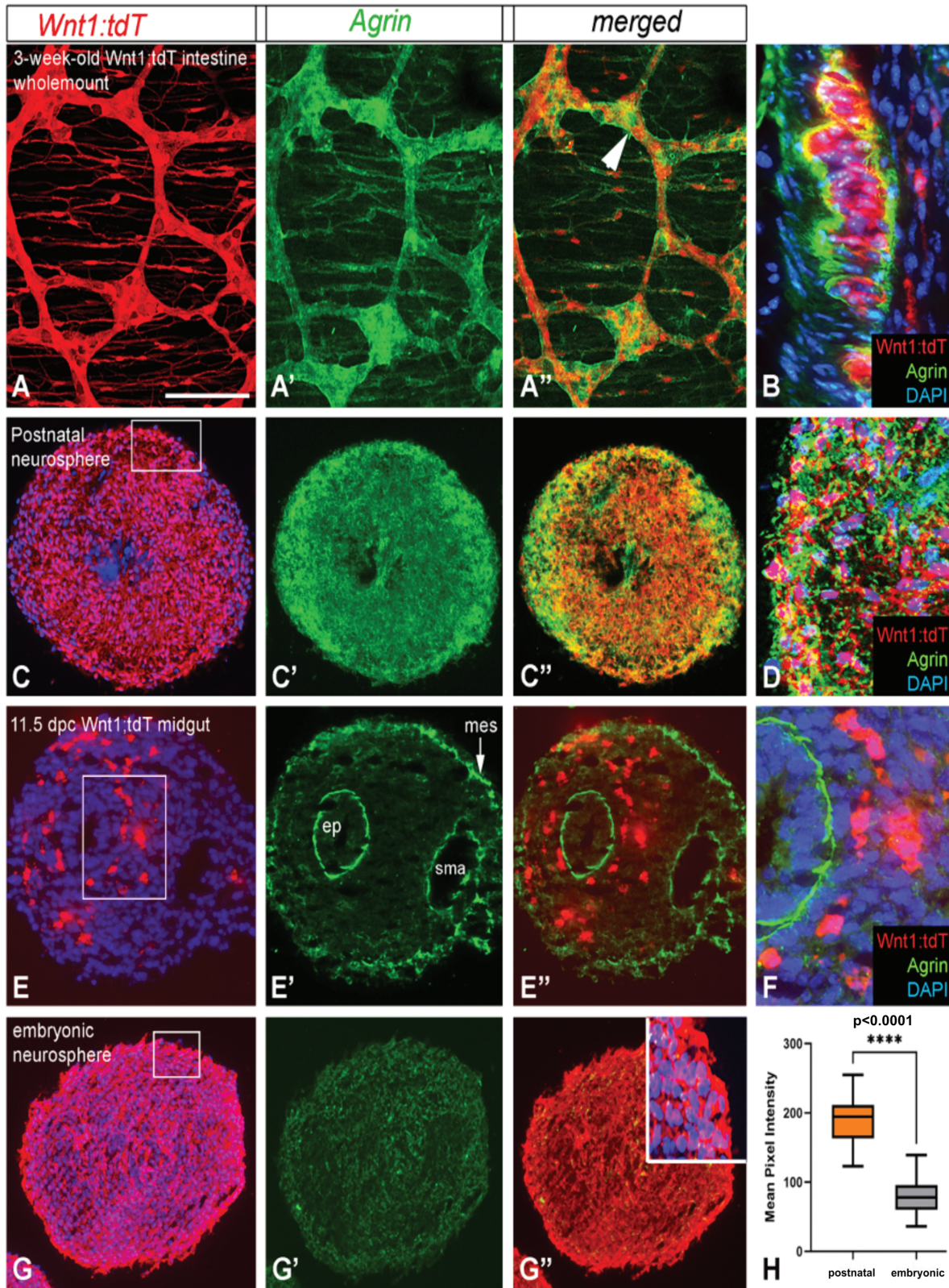


Figure 2. Agrin expression is significantly higher in postnatal as compared to embryonic neurospheres. Wholemount LMMP from 3-week old Wnt1:tdT mice reveals agrin expression in the myenteric plexus (A). Arrow in A' indicates myenteric ganglia sectioned. Validation of agrin specificity to enteric plexus of postnatal mice by labeling with Wnt1:tdT (B). Neurospheres derived from these mice show strong agrin expression (C). Boxed area magnified in D. In contrast, midgut from E11.5 Wnt1:tdT mice reveals markedly decreased agrin expression (E, boxed area magnified in F), as do enteric neurospheres derived from that tissue (G, boxed area magnified in G'' inset). Quantification of mean pixel intensity of Agrin immunoreactive cells (H). Scale bar in A applies to all other panels: 150 μ m (A,C); 70 μ m (B); 45 μ m (D); 100 μ m (F); 145 μ m (G); 70 μ m (G, inset). ep, epithelium; mes, mesothelial cells; sma, superior mesenteric artery.

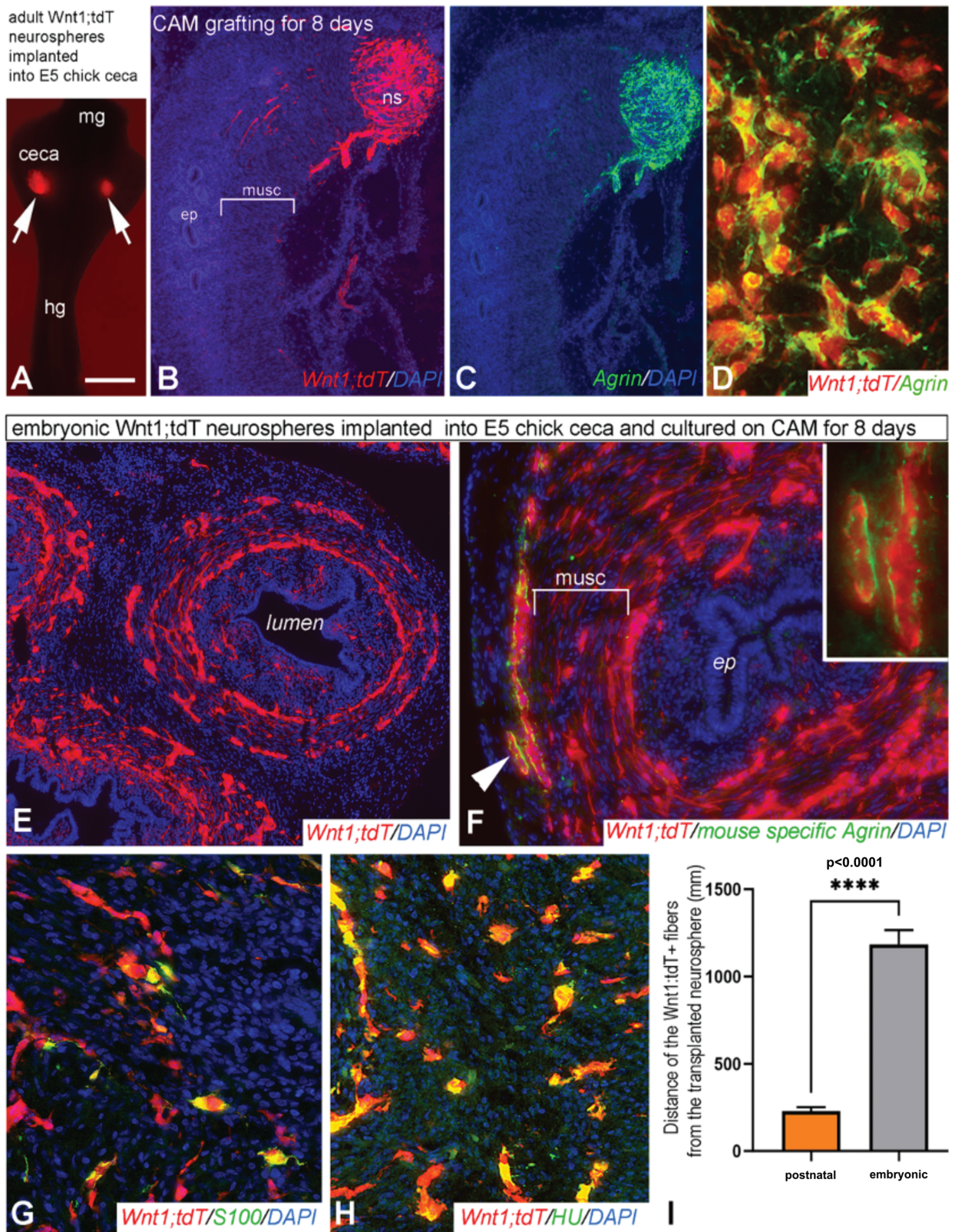


Figure 3. ENDCC migration is markedly diminished in postnatal neurospheres. Postnatal-derived neurospheres from 3-week old Wnt1;tdT mice were implanted into chick ceca and then grafted onto the CAM of host chick embryos (A). Wnt1 + ENDCCs (B) express agrin (C) and exhibit limited cell migration (B). A higher power view reveals expression of agrin by Wnt1;tdT + cells (D). A similar experiment using embryonic neurospheres from E11.5 Wnt1;tdT mice (E) reveals minimal agrin expression (F) and robust tdT + ENDCC migration (E). Immunostaining of transplanted Wnt1 + ENDCCs shows differentiation of transplanted cells into glia (S100+) (G) and neurons (HU+) (H). Quantification of the length (μm) of Wnt1;tdT + fibers and cells migrating from the transplanted neurosphere (I). Scale bar in A applies to all other panels: 350 μm (A), 175 μm (B,C), 15 μm (D), 150 μm (E), 100 μm (F), 50 μm (G), 70 μm (H). ep, epithelium; hg, hindgut; mg, midgut; musc, muscularis propria; ns, neurosphere; sma, superior mesenteric artery.

function-blocking antibody (20 $\mu\text{g}/\text{mL}$, Fig. 4B) for 72 hours. Agrin blockade led to a significant increase in ENCDC migration by 114% when compared to control conditions (283 676 μm^2 vs 132,854 μm^2 , respectively, $P < 0.001$, Fig. 4C, Supplementary Table S2).

Agrin Blockade Increases Proportion of GFAP-Expressing Cells But Has No Effect on ENCDC Proliferation

Sorted tdT + neurospheres derived from 4-12 week-old Wnt1;tdT mice were grown on fibronectin and cultured in the presence or absence of agrin function-blocking antibody (20 $\mu\text{g}/\text{mL}$). After 72 hours, neurospheres were treated for 24 hours with 10 μM EdU to assess cell proliferation. Given that agrin inhibition significantly enhanced migration, we wanted to assess cell differentiation and proliferation alongside a migration assay and therefore examined differentiation after 96 hours of 2-dimensional cell growth on fibronectin rather than examining 3-dimensional neurospheres in culture.

Agrin inhibition significantly increased the proportion of cells expressing GFAP (12.1% vs 6.4%, $P = .05$, Fig. 5A), but had no effect on differentiation into neurons expressing nNOS (17.4% vs 15.1%, $P = 0.44$, Fig. 5B) or Calretinin (CR) + (8.2% vs 8.3%, $P = .93$, Fig. 5C).

Cells expressing GFAP, which labels both enteric glia and ENCDC progenitors, migrated significantly farther (505% farther) in neurospheres treated with agrin inhibition (305.0 vs 50.4 μm , $P < .0001$). Agrin inhibition also improved migration of Calretinin + and nNOS + cells, although to a much lesser degree. nNOS + cells treated with agrin inhibition migrated 154% farther than control (239.0 vs 94.0 μm , $P < .0001$), and Calretinin + cells treated with agrin inhibition migrated 77% farther (105.8 vs 60.2 μm , $P = 0.39$, Fig. 5D). Additionally, amongst the cells treated with agrin inhibition, both GFAP + cells and nNOS + cells migrated farther than Calretinin + cells (GFAP + 304.7 μm vs Calretinin + 105.8 μm , $P < 0.0001$, nNOS + 239.0 μm vs Calretinin + 105.8 μm , $P = 0.0002$).

Inhibition of agrin had no effect on ENCDC proliferation, with 6.8% of Wnt1;tdT + cells in the neurospheres treated

with agrin function-blocking antibody expressing EdU versus 9.6% of Wnt1;tdT + cells in control neurospheres (Fig. 5E, $P = .50$).

Agrin Blockade Increases the Length of Neurite Projections

Neurospheres generated from adult Baf53b-Cre; R26tdT mice were plated on fibronectin with or without the presence of agrin antibody. This mouse model was chosen because Baf53b is a known marker of nerve fibers^{55,56} and therefore all nerve fibers are marked by tdT fluorescence, highlighting the effect of agrin inhibition on neurite projection. After 1 week, the cells were imaged and the longest 5 neurites per image were averaged. Average neurite length was compared between the 2 groups (Fig. 5F). Neurospheres cultured in proliferation media alone (Fig. 5G) had shorter projections than those supplemented with agrin antibody (Fig. 5H) (365 vs 750 μm , respectively, $P = .006$).

Neurospheres Expressing Agrin shRNA Exhibit Increased Cellular Migration Following Transplantation

Neurospheres were transduced with control lentivirus expressing scrambled shRNA (Supplementary Fig. S2A) or with agrin shRNA lentivirus (Supplementary Fig. S2B). Three days after transduction, strong TUJ1 expression confirms the presence of enteric neurons throughout the neurospheres (Supplementary Fig. 2C, 2D). While control neurospheres continue to express agrin (Supplementary Fig. 2E), transduction with agrin shRNA lentivirus led to successful silencing of its expression (Supplementary Fig. 2F).

Transduced neurospheres were transplanted onto ex vivo organ cultures of the colon obtained from wild-type C57/B6 mice and maintained for 7 days. When compared to control neurospheres (Fig. 6A), agrin shRNA neurospheres (Fig. 6B) exhibited 57% farther migration of Wnt1;tdT + cells compared to control neurospheres (592 794 μm^2 vs 378 282 μm^2 ; $P = .05$, Fig. 6C, Supplementary Table S2). This experiment was repeated using aganglionic colon explants obtained from *Ednrb*^{-/-} mice, a commonly used model of human Hirschsprung disease.⁵⁷ We observed a trend

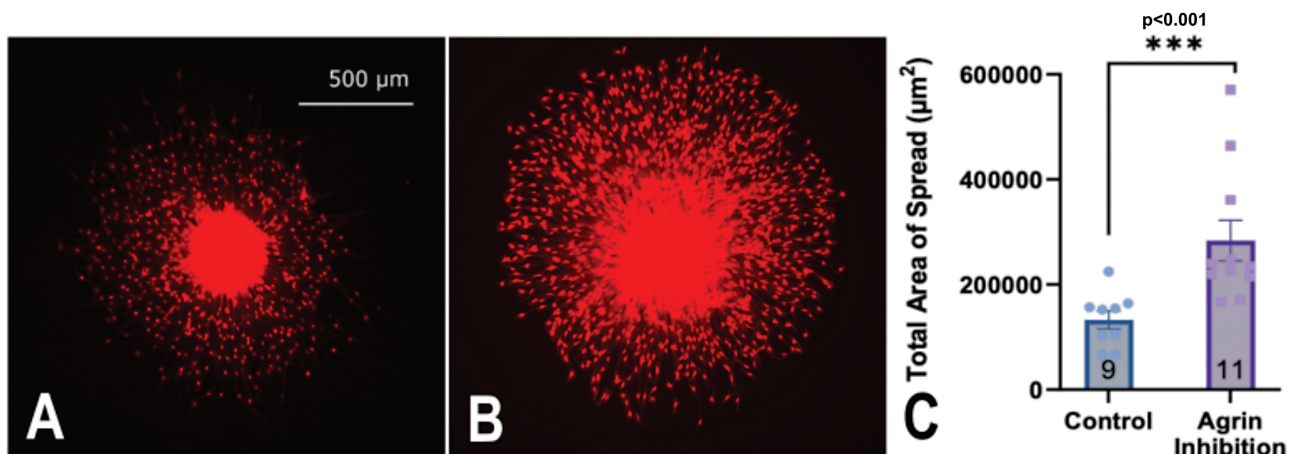


Figure 4. Agrin inhibition promotes cell migration from neurospheres in vitro. Enteric neurospheres derived from adult Wnt1;tdT mice were sorted for tdT expression and cultured on fibronectin for 72 hours. Control neurospheres show limited outward migration of cells from the neurosphere (A) as compared to those treated with an agrin function-blocking antibody (B). Bar graph of total area of cell spread (μm^2) with SEM bars shows that agrin inhibition significantly enhances cell migration (C). Scale bar in A applies to panels A and B.

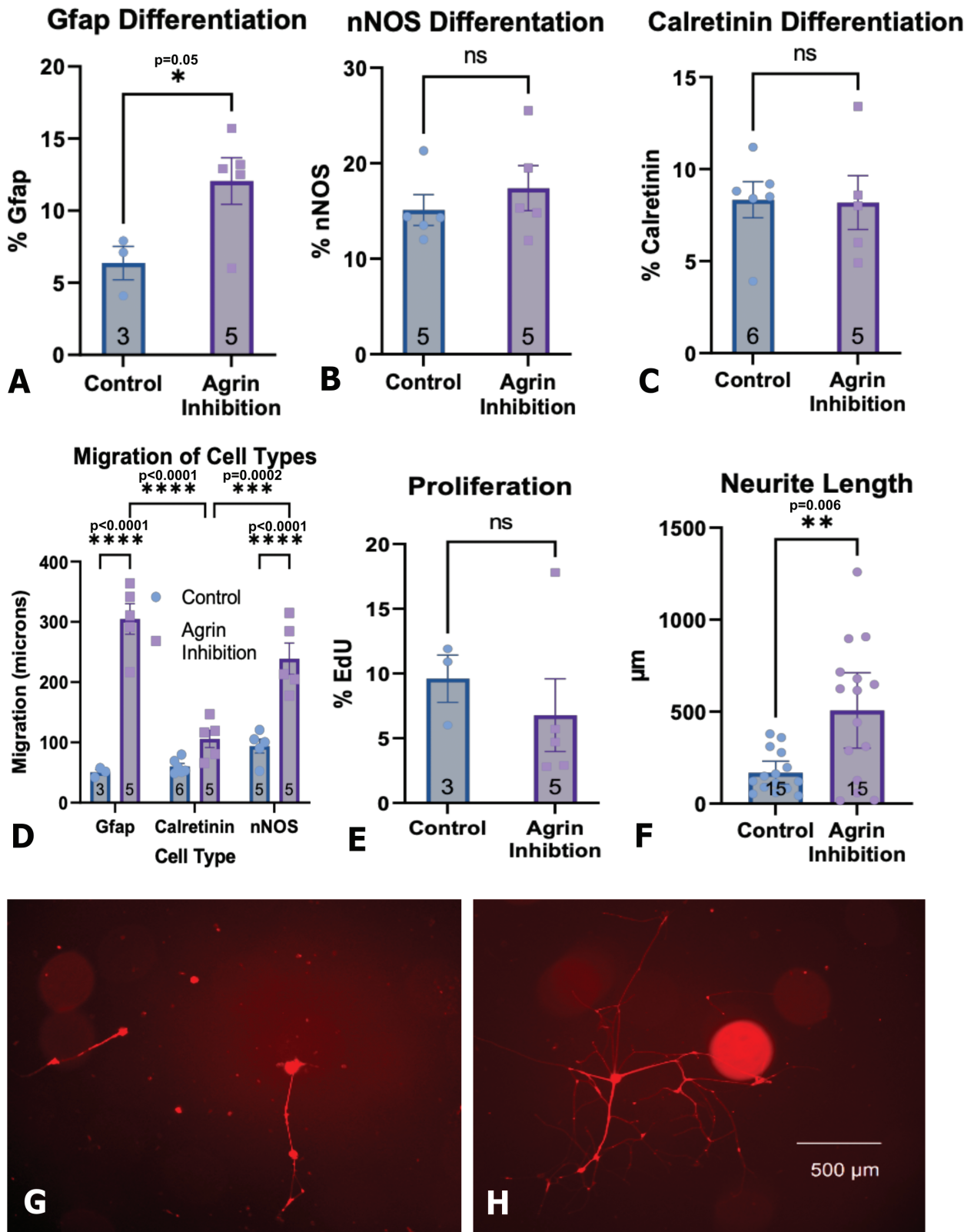


Figure 5. Agrin inhibition promotes Gfap differentiation but has no effect on proliferation. Enteric neurospheres derived from adult Wnt1;tdT mice were sorted for tdT expression and cultured on fibronectin for 96 hours. A subset was treated with EdU after 72 hours, 24 hours prior to fixation. Neurospheres treated with agrin function-blocking antibody demonstrate increased GFAP + differentiation (A), but no change in nNOS (B) or Calretinin (C) differentiation. All cells, including GFAP+, Calretinin+, and nNOS + migrated further when treated with agrin inhibition (D), although the greatest change was observed for GFAP + cells. Agrin inhibition also had no effect on cell proliferation (E). Agrin inhibition increased the length of neurite projections (F) as shown with neurospheres from Baf53b;tdT mice grown in control media (G) or media supplemented with agrin antibody (H).

toward increased migration of neurospheres transduced with agrin shRNA lentivirus versus controls, with agrin inhibition associated with 46% greater migration, although this did not reach statistical significance ($205\,241\ \mu\text{m}^2$ vs $121\,436\ \mu\text{m}^2$; $P = 0.24$, Fig. 6D, Supplementary Table S2). Interestingly, transplanted cell migration is significantly less in the aganglionic colon versus the ganglionic colon. This has been observed previously,² and we hypothesize is at least partially due to a non-permissive ECM, but further research is needed. Note that the recipient explant tissue was stained for Tuj1 to confirm the presence of aganglionosis (Fig. 6E).

Finally, we performed in vivo transplants to determine whether agrin inhibition enhances ENCDC migration in this setting. Two neurospheres were implanted subserosally approximately 0.5 cm apart in the distal colon of wild-type C57/B6 mice (Fig. 7A, 7B) via laparotomy. The transplanted segment of the colon was harvested 7 days later. An example of stained tissue is shown in Fig. 7C, where Wnt1;tdT marks the transplanted cells, TUJ1 stains nerve fibers, and GFP represents the reporter from the lentivirus. In comparison to control neurospheres (Fig. 7D), neurospheres transduced with agrin shRNA lentivirus (Fig. 7E) migrated 43% farther than control neurospheres, and this difference was statistically significant ($316\,856\ \mu\text{m}^2$ vs $222\,330\ \mu\text{m}^2$; $P = 0.03$, Fig. 7E, Supplementary Table S2).

Discussion

ENCDCs actively modify their extracellular matrix as they migrate along the gut mesenchyme.¹¹ As a consequence, in Hirschsprung disease not only are the enteric ganglia absent in the aganglionic segment, but the surrounding extracellular matrix is also altered. ENCDCs secrete many ECM molecules, including tenascin-C,⁹ collagen 18, and agrin,¹¹ at various time points along their embryonic journey from the neural tube to the colorectum to regulate their migration. Importantly, agrin, which is inhibitory to ENCDC migration, is not expressed at the migratory wavefront or by ENS progenitor cells but rather is expressed by trailing ENCDCs, which have completed the migration and initiated neuroglial differentiation.^{11,58} For regenerative cell therapy to be successful as a treatment for neurointestinal diseases, this altered matrix must be considered and modified in order to maximize its permissiveness. This can be best accomplished by directly modifying the donor stem cells to mirror the interactions between ENCDCs and their ECM environment during embryonic ENS formation. Our study is the first to perform a comprehensive comparison of the transcriptome between migrating embryonic progenitor cells and the cells that comprise the therapeutic product in stem cell therapy, namely enteric neurospheres. We identified 89 ECM-associated genes that are differentially expressed between postnatal enteric neurospheres and embryonic ENCDC

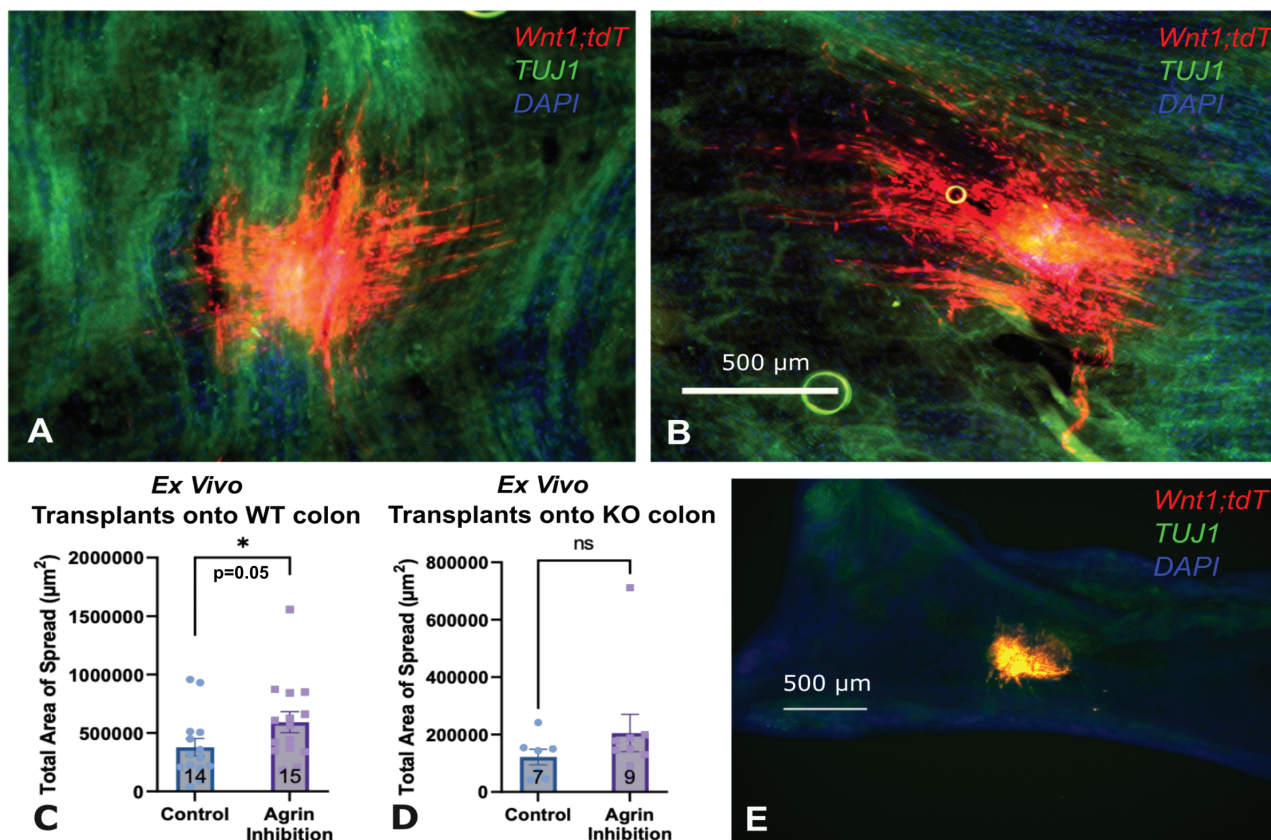


Figure 6. Agrin inhibition in neurospheres enhances cell migration following ex vivo transplantation. Immunostaining of LMMP of wild-type mouse colon 7 days after ex vivo transplantation of adult Wnt1;tdT control neurospheres (A) shows significantly less migration of tdT-expressing cells as compared to transplantation of neurospheres expressing agrin-shRNA lentivirus (B, C). Ex vivo transplantation of control neurospheres onto colonic tissue obtained from 2-week-old *Ednr^{b-/-}* mice reveals a trend toward decreased migration of tdT-expressing cells as compared to transplantation of neurospheres expressing agrin-shRNA lentivirus (D). Immunostaining of Wnt1 + transplanted cells on KO tissue for TUJ1 confirms aganglionosis (E).

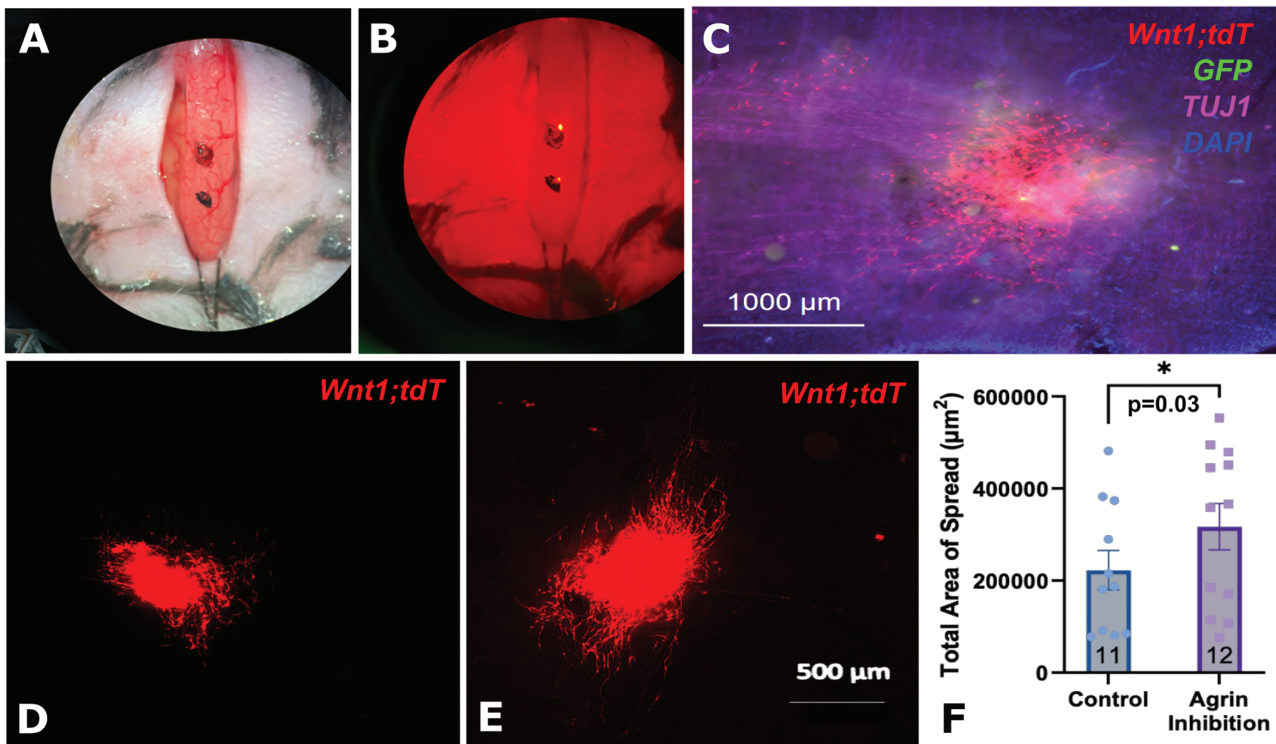


Figure 7. Silencing of agrin expression in neurospheres significantly improves cell migration following transplantation in vivo. Two neurospheres were implanted subserosally into the distal colon of wild-type mice (A), with tdT fluorescence confirming proper placement (B). LMMP of wild-type mouse colon was examined 7 days after in vivo transplantation (C), where Wnt1;tdT marks the transplanted cells, TUJ1 stains intrinsic and transplanted nerve fibers, and GFP represents the reporter in the lentivirus. Adult Wnt1;tdT control neurospheres (D) migrating significantly less than neurospheres expressing agrin-shRNA lentivirus (E, F).

progenitors. Specifically, we found that agrin is highly over-expressed by neurospheres, which is problematic given its known inhibitory role on ENCDC migration. While we focused on agrin, this set of 89 differentially expressed ECM genes includes many potential targets for stem cell modification to enhance the success of cell therapy and should serve as a resource for further research.

Agrin is a large HSPG widely expressed in the developing brain and in the basal lamina of developing tissues. In the central nervous system, it is involved in synaptogenesis, plasticity, and signaling.⁵⁹ Its role in the ENS is less well understood, but it has been shown to be expressed as part of an ECM capsule surrounding the myenteric ganglia and has been hypothesized to have a role in barrier function.⁶⁰ The expression of agrin around the ganglia persists postnatally and therefore may be important in ENS maintenance.¹¹ Agrin plays an important role in development and has been shown to inhibit retinal neurite outgrowth in vitro⁵⁴ and, as described above, to inhibit migration of ENCDCs.¹¹ We therefore hypothesized that agrin inhibition in neurospheres would enhance cell migration following transplantation.

Agrin is found throughout the body in multiple forms. Secreted agrin is widely expressed in various tissues, whereas a transmembrane form is primarily expressed in the brain.⁵⁹ Agrin is expressed and secreted by ENCDCs but also by the cells in the surrounding ECM. In this study, we specifically focused on modifying the agrin produced by ENCDCs, not the agrin present in the host environment. When neurospheres were cultured on fibronectin alone, there was no ECM agrin in this culture. The anti-agrin antibody is therefore blocking agrin produced by the neural crest-derived cells. In the

ex vivo and in vivo assays where there is likely to be pre-existing agrin in the surrounding ECM, we utilized shRNA to specifically silence the agrin production by cells within the neurosphere.

We found that agrin is highly expressed by neurospheres derived from the postnatal intestine, but not those from the embryonic gut, consistent with our single-cell transcriptional analysis. Following transplantation into avian ceca, embryonic neurospheres migrate significantly farther than neurospheres generated from postnatal intestine, likely due, at least in part, to the absence of agrin expression. By using a function-blocking antibody or an agrin shRNA lentiviral vector, we show that agrin inhibition increases ENCDC migration from neurospheres following in vitro, ex vivo, and in vivo transplantation.

We repeated the ex vivo experiment on colonic organ cultures from both wild-type and *Ednrb*^{-/-} mice to test whether agrin inhibition could enhance cell migration in the aganglionic intestine. We opted to test this in organotypic cultures since in vivo experiments in this knock-out model are challenging due to their limited lifespan of 3-4 weeks. Although the effect of agrin inhibition in aganglionic colon from Hirschsprung mice did not achieve statistical significance, the direction and magnitude of change were similar to that in wild-type tissue, suggesting the presence of a comparable effect. ENCDC migration following cell transplantation is known to be reduced in aganglionic intestine,² possibly related to the presence of multiple differences in matrix protein expression. We hypothesize that modification of more than one ECM protein may be necessary to significantly enhance migration in that environment.

The mechanism through which agrin inhibits cell migration is largely unknown. Agrin has two known receptors, the muscle-specific receptor tyrosine kinase MuSK and the cell surface receptor dystroglycan. Agrin represents a ligand for MuSK and its obligate co-receptor LPR4 at the neuromuscular junction.⁶¹ MuSK is expressed by smooth muscle cells in the gut, but not by the ENS.¹¹ In contrast, dystroglycan is a cell surface receptor that interacts with numerous ECM proteins,⁶² including laminin and agrin, and is expressed by ENCDCs and enteric ganglia.¹¹ Prior work hypothesized that when ENCDCs have reached their target location they secrete agrin, which then binds the cell surface receptor dystroglycan, and signals for the cell to stop migrating.¹¹

Inhibition of migration can also be an indirect consequence of alterations in cell proliferation and differentiation. While we did not observe an effect on proliferation, we found that agrin inhibition significantly increased the proportion of GFAP-expressing cells without affecting nNOS or calretinin populations. Importantly, GFAP marks both enteric glial cells and neuronal progenitor cells.^{47,63,64} We therefore hypothesize that agrin inhibition may specifically help maintain the pool of GFAP + progenitors. Interestingly, the effect of agrin inhibition on promoting cell migration was particularly profound on the GFAP-expressing cells, suggesting that this population may be especially migratory, though further studies are needed.

Conclusion

While others have co-administered stem cells alongside nanoparticles to enhance their effect,⁴¹ or used lentiviral vectors to label cells prior to transplantation,^{2,65} our study is the first to directly modify stem cells for the treatment of ENS disease. Stem cell modification represents a promising tool for ENS regenerative therapy, one that has been actively applied in studies on spinal cord injury,⁶⁶⁻⁶⁸ but not yet on neurointestinal diseases. We have shown that modification of enteric neuronal stem cells via agrin inhibition can significantly improve their success following transplantation into the gut.

Funding

J.L.M. was supported by F32DK131792 and A.M.G. was supported by R01DK119210. N.N. is supported by the Research Excellence Programme of the ITM in Hungary, within the framework of the TKP2021-EGA-25 thematic program of Semmelweis University; and by a Hungarian Science Foundation NKFI grant K-138664.

Conflict of Interests

A.G. declared research funding from NIH. The other authors declared no potential conflicts of interest.

Author Contributions

J.L.M.: conception and design, assembly of data, data analysis, manuscript writing. R.S.: assembly of data, data analysis, final approval of manuscript. R.A.G., A.S., S.B., C.H.: data analysis, final approval of manuscript. R.H., N.N.: conception and design, assembly of data, manuscript writing. A.M.G.: conception and design, manuscript writing.

Data Availability

The data underlying this article will be shared on reasonable request to the corresponding author.

Supplementary Material

Supplementary material is available at *Stem Cells Translational Medicine* online.

References

- Cheng LS, Hotta R, Graham HK, et al. Postnatal human enteric neuronal progenitors can migrate, differentiate, and proliferate in embryonic and postnatal aganglionic gut environments. *Pediatr Res.* 2017;81(5):838–846. <https://doi.org/10.1038/pr.2017.4>
- Hotta R, Cheng L, Graham H, et al. Isogenic enteric neural progenitor cells can replace missing neurons and glia in mice with Hirschsprung disease. *Neurogastroenterol Motil.* 2016;28(4):498–512.
- Lindley RM, Hawcutt DB, Connell MG, et al. Human and mouse enteric nervous system neurosphere transplants regulate the function of aganglionic embryonic distal colon. *Gastroenterology.* 2008;135(1):205–216.e6. <https://doi.org/10.1053/j.gastro.2008.03.035>
- Hotta R, Stamp LA, Foong JPP, et al. Transplanted progenitors generate functional enteric neurons in the postnatal colon. *J Clin Invest.* 2013;123(3):1182–1191. <https://doi.org/10.1172/JCI65963>
- Hetz S, Acikgoez A, Voss, et al. In vivo transplantation of neurosphere-like bodies derived from the human postnatal and adult enteric nervous system: a pilot study. *PLoS One.* 2014;9(4):e93605. <https://doi.org/10.1371>
- Nagy N, Goldstein AM. Enteric nervous system development: a crest cell's journey from neural tube to colon. *Seminars Cell Dev Biol.* 2017;66:94–106. <https://doi.org/10.1016/j.semcdb.2017.01.006>
- Nagy N, Mwirerwa O, Karina Y, et al. Endothelial cells promote migration and proliferation of enteric neural crest cells via beta1 integrin signaling. *Dev Biol.* 2009;330(2):263–272.
- Yasui Y, Yoshizaki H, Kuwahara T, et al. Transplanted neural crest cells migrate toward Auerbach's plexus layer instead of the colon surface in recipient colon pretreated with collagenase and fibronectin. *Biochem Biophys Res Commun.* 2022;601(601):116–122. <https://doi.org/10.1016/j.bbrc.2022.02.094>
- Akbareian SE, Nagy N, Steigher CE, et al. Enteric neural crest-derived cells promote their migration by modifying their microenvironment through tenascin-C production. *Dev Biol.* 2013;382(2):446–456.
- Breau MA, Dahmani A, Broders-Bondon F, Thiery JP, Dufour S. Beta1 integrins are required for the invasion of the caecum and proximal hindgut by enteric neural crest cells. *Development.* 2009;136(16):2791–2801. <https://doi.org/10.1242/dev.031419>
- Nagy N, Barad C, Hotta R, et al. Collagen 18 and agrin are secreted by neural crest cells to remodel their microenvironment and regulate their migration during enteric nervous system development. *Development.* 2018;145(9):dev160317. <https://doi.org/10.1242/dev.160317>
- Broders-Bondon F, Paul-Gilloteaux P, Carlier C, Radice GL, Dufour S. N-cadherin and β 1-integrins cooperate during the development of the enteric nervous system. *Dev Biol.* 2012;364(2):178–191. <https://doi.org/10.1016/j.ydbio.2012.02.001>
- Soret R, Mennetrey M, Bergeron KF, et al; Ente-Hirsch Study Group. A collagen VI-dependent pathogenic mechanism for Hirschsprung's disease. *J Clin Invest.* 2015;125(12):4483–4496. <https://doi.org/10.1172/JCI83178>
- Nagy N, Barad C, Graham HK, et al. Sonic hedgehog controls enteric nervous system development by patterning the extracellular matrix. *Development.* 2016;143(2):264–275. <https://doi.org/10.1242/dev.128132>

15. Ring C, Hassell JR, Halfter W. Expression pattern of collagen IX and potential role in the segmentation of the peripheral nervous system. *Dev Biol.* 1996;180(1):41–53. <https://doi.org/10.1006/dbio.1996.0283>
16. Dutt S, Kléber M, Matasci M, Sommer L, Zimmermann DR. Versican V0 and V1 guide migratory neural crest cells. *J Biol Chem.* 2006;281(17):12123–12131. <https://doi.org/10.1074/jbc.M510834200>
17. Perris R, Perissinotto D, Pettway Z, et al. Inhibitory effects of PG-H/aggrecan and PG-M/versican on avian neural crest cell migration. *FASEB J.* 1996;10(2):293–301. <https://doi.org/10.1096/fasebj.10.2.8641562>
18. Mueller, Jessica L, Goldstein AM. The science of Hirschsprung disease: what we know and where we are headed. *Semin Pediatr Surg.* 2022;31(2):151157.
19. Goldstein AM, Thapar N, Karunaratne TB, De Giorgio R. Clinical aspects of neurointestinal disease: pathophysiology, diagnosis, and treatment. *Dev Biol.* 2016;417(2):217–228. <https://doi.org/10.1016/j.ydbio.2016.03.032>
20. Westfal ML, Goldstein AM. Pediatric enteric neuropathies: diagnosis and current management. *Curr Opin Pediatr.* 2017;29(3):347–353.
21. Langer JC, Durrant AC, de la Torre L, et al. One-stage transanal soave pullthrough for hirschsprung disease: a multicenter experience with 141 children. *Ann Surg.* 2003;238(4):569–583. <https://doi.org/10.1097/01.sla.0000089854.00436.cd>
22. Zimmer J, Tomuschat C, Puri P. Long-term results of transanal pull-through for Hirschsprung's disease: a meta-analysis. *Pediatr Res.* 2016;32(8):743–749. <https://doi.org/10.1007/s00383-016-3908-z>
23. Neuvonen MI, Kyrklund K, Lindahl HG, et al. A population-based, complete follow-up of 145 consecutive patients after transanal mucosectomy for Hirschsprung disease. *J Pediatr Surg.* 2015;50(10):1653–1658. <https://doi.org/10.1016/j.jpedsurg.2015.02.006>
24. Mc Laughlin D, Friedmacher F, Puri P. Total colonic aganglionosis: a systematic review and meta-analysis of long-term clinical outcome. *Pediatr Surg Int.* 2012;28(8):773–779.
25. Catto-Smith AG, Trajanovska M, Taylor RG. Long-term continence after surgery for Hirschsprung's disease. *J Gastroenterol Hepatol.* 2007;22(12):2273–2282. <https://doi.org/10.1111/j.1440-1746.2006.04750.x>
26. Jarvi K, Laitakari EM, Koivusalo A, Rintala RJ, Pakarinen MP. Bowel function and gastrointestinal quality of life among adults operated for Hirschsprung disease during childhood: a population-based study. *Ann Surg.* 2010;252(6):977–981. <https://doi.org/10.1097/SLA.0b013e3182018542>
27. Niramis R, Watanatittan S, Anuntkosol M, et al. Quality of life of patients with Hirschsprung's disease at 5-20 years post pull-through operations. *Eur J Pediatr Surg* 2008;18(1):38-43.
28. Cheng LS, Graham HK, Pan WH, et al. Optimizing neurogenic potential of enteric neurospheres for treatment of neurointestinal diseases. *J Surg Res.* 2016;206(2):451-459. <https://doi.org/10.1016/j.jss.2016.08.035>
29. Metzger M, Caldwell C, Barlow AJ, Burns AJ, Thapar N. Enteric nervous system stem cells derived from human gut mucosa for the treatment of aganglionic gut disorders. *Gastroenterology.* 2009;136(7):2214–25.e1. <https://doi.org/10.1053/j.gastro.2009.02.048>
30. Almond S, Lindley R, Kenny SE, Connell MG, Edgar DH. Characterisation and transplantation of enteric nervous system progenitor cells. *Gut.* 2007;56(4):489–496.
31. Rauch U, Hänsgen A, Hagl C, Holland-Cunz S, Schäfer KH. Isolation and cultivation of neuronal precursor cells from the developing human enteric nervous system as a tool for cell therapy in dysganglionosis. *Int J Colorectal Dis.* 2006;21(6):554–559. <https://doi.org/10.1007/s00384-005-0051-z>
32. Metzger M, Bareiss PM, Danker T, et al. Expansion and differentiation of neural progenitors derived from the human adult enteric nervous system. *Gastroenterology.* 2009;137(6):2063–2073.e4. <https://doi.org/10.1053/j.gastro.2009.06.038>
33. Wilkinson DJ, Bethell GS, Shukla R, Kenny SE, Edgar DH. Isolation of enteric nervous system progenitor cells from the aganglionic gut of patients with Hirschsprung's disease. *PLoS One.* 2015;10(5):e0125724. <https://doi.org/10.1371>
34. Lindley RM, Hawcutt DB, Connell MG, Edgar DH, Kenny SE. Properties of secondary and tertiary human enteric nervous system neurospheres. *J Pediatr Surg.* 2009;44(6):1249–1255. <https://doi.org/10.1016/j.jpedsurg.2009.02.048>
35. Bondurand N, Natarajan D, Thapar N, Atkins C, Pachnis V. Neuron and glia generating progenitors of the mammalian enteric nervous system isolated from foetal and postnatal gut cultures. *Development.* 2003;130(25):6387–6400. <https://doi.org/10.1242/dev.00857>
36. Hotta R, Anderson RB, Kobayashi K, Newgreen DF, Young HM. Effects of tissue age, presence of neurones and endothelin-3 on the ability of enteric neurone precursors to colonize recipient gut: implications for cell-based therapies. *Neurogastroenterol Motil.* 2010;22(3):331–e86. <https://doi.org/10.1111/j.1365-2982.2009.01411.x>
37. Druckenbrod NR, Epstein ML. Age-dependent changes in the gut environment restrict the invasion of the hindgut by enteric neural progenitors. *Development.* 2009;136(18):3195–3203. <https://doi.org/10.1242/dev.031302>
38. Liu W, Yue W, Wu R. Overexpression of Bcl-2 promotes survival and differentiation of neuroepithelial stem cells after transplantation into rat aganglionic colon. *Stem Cell Res Ther.* 2013;4(1):7. <https://doi.org/10.1186/scrt155>
39. Liu W, Zhang L, Wu R. Enteric neural stem cells expressing insulin-like growth factor 1: a novel cellular therapy for Hirschsprung's disease in mouse model. *DNA Cell Biol.* 2018;37(7):642–648. <https://doi.org/10.1089/dna.2017.4060>
40. Micci MA, Pattillo MT, Kahrig KM, Pasricha PJ. Caspase inhibition increases survival of neural stem cells in the gastrointestinal tract. *Neurogastroenterol Motil.* 2005;17(4):557–564. <https://doi.org/10.1111/j.1365-2982.2005.00702.x>
41. Hotta R, Cheng LS, Graham HK, et al. Delivery of enteric neural progenitors with 5-HT4 agonist-loaded nanoparticles and thermosensitive hydrogel enhances cell proliferation and differentiation following transplantation in vivo. *Biomaterials.* 2016;88:1–11. <https://doi.org/10.1016/j.biomaterials.2016.02.016>
42. Mallapragada SK, Brenza TM, McMillan JM, et al. Enabling nanomaterial, nanofabrication and cellular technologies for nanoneurotherapeutics. *Nanomedicine.* 2015;11(3):715–729. <https://doi.org/10.1016/j.nano.2014.12.013>
43. Parikh D, Tam P, Van Velzen D, Edgar D. Abnormalities in the distribution of laminin and collagen type IV in Hirschsprung's disease. *Gastroenterology.* 1992;102(4):1236–1241. [https://doi.org/10.1016/0016-5085\(92\)70018-7](https://doi.org/10.1016/0016-5085(92)70018-7)
44. Parikh D, Tam P, Van Velzen D, Edgar D. The extracellular matrix components, tenascin and fibronectin, in Hirschsprung's disease: an immunohistochemical study. *J Pediatr Surg.* 1994;29(10):1302–1306. [https://doi.org/10.1016/0022-3468\(94\)90101-5](https://doi.org/10.1016/0022-3468(94)90101-5)
45. Gao N, Wang J, Zhang Q, et al. Aberrant distributions of collagen I, III, and IV in Hirschsprung disease. *J Pediatr Gastroenterol Nutr.* 2020;70(4):450–456. <https://doi.org/10.1097/MPG.0000000000002627>
46. Morarach K, Mikhailova A, Knoflach V, et al. Diversification of molecularly defined myenteric neuron classes revealed by single-cell RNA sequencing. *Nat Neurosci.* 2021;24(1):34–46. <https://doi.org/10.1038/s41593-020-00736-x>
47. Guyer RA, Stavely R, Robertson K, et al. Single-cell multiome sequencing clarifies enteric glial diversity and identifies an intraganglionic population poised for neurogenesis. *Cell Rep.* 1121;42(3):94.
48. Stuart T, Butler A, Hoffman P, et al. Comprehensive integration of single-cell data. *Cell.* 2019;177(7):1888–1902.e21. <https://doi.org/10.1016/j.cell.2019.05.031>

49. Blondel VD, Guillaume JL, Lambiotte R, Lefebvre E. Fast unfolding of communities in large networks. *J Stat Mech.* 2008;2008(10):P10008.
50. Love MI, Huber W, Anders S. Moderated estimation of fold change and dispersion for RNA-seq data with DESeq2. *Genome Biol.* 2014;15(12):550. <https://doi.org/10.1186/s13059-014-0550-8>
51. Southwell BR. Staging of intestinal development in the chick embryo. *Anatom Record Part A Discov Mole, Cellul Evoluti Biol.* 2006;288A(8):909–920. <https://doi.org/10.1002/ara.20349>
52. Nagy N, Burns AJ, Goldstein AM. Immunophenotypic characterisation of enteric neural crest cells in the developing avian colorectum. *Dev Dyn.* 2012;241(5):842–851.
53. Fu M, Barlow-Anacker AJ, Kuruvilla KP, et al. 37/67-Laminin receptor facilitates neural crest cell migration during enteric nervous system development. *FASEB J.* 2020;34(8):10931–10947. <https://doi.org/10.1096/fj.202000699R>
54. Halfter W, Schurer B, Yip J, et al. Distribution and substrate properties of agrin, a heparan sulfate proteoglycan of developing axonal pathways. *J Comp Neurol.* 1997;383(1):1–17.
55. Zhan X, Cao M, Yoo AS, et al. Generation of BAF53b-Cre transgenic mice with pan-neuronal Cre activities. *Genesis.* 2015;53(7):440–448. <https://doi.org/10.1002/dvg.22866>
56. Stavely R, Hotta R, Picard N, et al. Schwann cells in the subcutaneous adipose tissue have neurogenic potential and can be used for regenerative therapies. *Sci Transl Med.* 2022;14(646):eabl8753. <https://doi.org/10.1126/scitranslmed.abl8753>
57. Hosoda K, Hammer RE, Richardson JA, et al. Targeted and natural (Piebald-Lethal) mutations of endothelin-B receptor gene produce megacolon associated with spotted coat color in mice. *Cell.* 1994;79(7):1267–1276. [https://doi.org/10.1016/0092-8674\(94\)90017-5](https://doi.org/10.1016/0092-8674(94)90017-5)
58. Stavely R, Hotta R, Guyer RA, et al. A distinct transcriptome characterizes neural crest-derived cells at the migratory wavefront during enteric nervous system development. *Development.* 2023;150(5):dev201090. <https://doi.org/10.1242/dev.201090>
59. Daniels MP. The role of Agrin in synaptic development, plasticity and signaling in the central nervous system. *Neurochem Int.* 2012;61(6):848–853. <https://doi.org/10.1016/j.neuint.2012.02.028>
60. Mogor F, Kovács T, Lohinai Z, Dora D. The enteric nervous system and the microenvironment of the gut: the translational aspects of the microbiome-gut-brain axis. *Appl Sci.* 2021;11(24):12000.
61. Zong Y, Jin R. Structural mechanisms of the Agrin-LRP4-MuSK signaling pathway in neuromuscular junction differentiation. *Cellul Mol Life Sci.* 2013;70(17):3077–3088. <https://doi.org/10.1007/s00018-012-1209-9>
62. Winder SJ. The complexities of dystroglycan. *Trends Biochem Sci.* 2001;26(2):118–124. [https://doi.org/10.1016/s0968-0004\(00\)01731-x](https://doi.org/10.1016/s0968-0004(00)01731-x)
63. Garcia ADR, Doan NB, Imura T, Bush TG, Sofroniew MV. GFAP-expressing progenitors are the principal source of constitutive neurogenesis in adult mouse forebrain. *Nat Neurosci.* 2004;7(11):1233–1241. <https://doi.org/10.1038/nn1340>
64. Liu Y, Namba T, Liu J, et al. Glial fibrillary acidic protein-expressing neural progenitors give rise to immature neurons via early intermediate progenitors expressing both glial fibrillary acidic protein and neuronal markers in the adult hippocampus. *Neuroscience.* 2010;166(1):241–251. <https://doi.org/10.1016/j.neuroscience.2009.12.026>
65. Natarajan D, Cooper J, Choudhury S, et al. Lentiviral labeling of mouse and human enteric nervous system stem cells for regenerative medicine studies. *Neurogastroenterol Motil.* 2014;26(10):1513–1518. <https://doi.org/10.1111/nmo.12420>
66. Jin Y, Ketschek A, Jiang Z, Smith G, Fischer I. Chondroitinase activity can be transduced by a lentiviral vector in vitro and in vivo. *J Neurosci Methods.* 2011;199(2):208–213. <https://doi.org/10.1016/j.jneumeth.2011.05.007>
67. Führmann T, Anandakumaran PN, Payne SL, et al. Combined delivery of chondroitinase ABC and human induced pluripotent stem cell-derived neuroepithelial cells promote tissue repair in an animal model of spinal cord injury. *Biomed Mater.* 2018;13(2):024103. <https://doi.org/10.1088>
68. Jevans B, James ND, Burnside E, et al. Combined treatment with enteric neural stem cells and chondroitinase ABC reduces spinal cord lesion pathology. *Stem Cell Res Ther.* 2021;12(1):10. <https://doi.org/10.1186/s13287-020-02031-9>